



ELSEVIER

Marine Micropaleontology 45 (2002) 291–307

MARINE
MICROPALAEONTOLOGY

www.elsevier.com/locate/marmicro

Miocene to Pliocene calcareous nannofossil biostratigraphy at ODP Leg 177 Sites 1088 and 1090

Maria Marino^{a,*}, José Abel Flores^b

^a Dipartimento di Geologia e Geofisica, Università di Bari, via E. Orabona 4, 70125 Bari, Italy

^b Universidad de Salamanca, Facultad de Ciencias, Departamento de Geología, 37008 Salamanca, Spain

Received 30 August 2000; accepted 7 August 2001

Abstract

The calcareous nannofossil biostratigraphy of ODP Leg 177 Sites 1088 and 1090 (Subantarctic sector from the Atlantic Ocean) is discussed. Most nannofossil zonal boundaries of Martini (1971) and Okada and Bukry (1980) were recognized for the studied mid–high-latitude sediments. Conventional low-latitude marker species such as *Amaurolithus* spp., *Discoaster* spp., *Triquetrorhabdulus* spp., *Ceratolithus* spp. were recorded as rare and scattered, which impeded the development of a detailed nannofossil biostratigraphic zonation of some Miocene and Pliocene intervals. Because of the absence of some primary biostratigraphic marker species, additional second-order bioevents, such as the first occurrence of *Calcidiscus macintyreii* and the last occurrence of *Coccolithus miopelagicus*, have been used to approximate the base of zones NN7 and NN8, respectively. Several disconformities disturbing the Pliocene and Miocene intervals of Site 1090 could be determined based on nannofossil distribution although the occurrence of intervals with dissolved nannofloras and low species diversity prevented a reliable age assignment. An acme of small *Gephyrocapsa* was recognized near the lower/middle Pliocene boundary, close to the NN15–NN16 zonal boundary, presenting an event for further improvement of the calcareous nannofossil biostratigraphy of this interval time. The first occurrence of *Pseudoemiliania lacunosa* ($> 4 \mu\text{m}$) occurs close to this interval, representing a fairly reliable event to approximate the base of NN15 zone when other biozonal events are absent. A paracme of *R. pseudoumbilicus* ($> 7 \mu\text{m}$) was detected in the lower Pliocene NN12 and in the upper Miocene NN11. These temporary absences of the species seem to be isochronous between high-latitude and low–middle-latitude areas. © 2002 Elsevier Science B.V. All rights reserved.

Keywords: Pliocene–Miocene; calcareous nannofossil biostratigraphy; Southern Ocean

1. Introduction

Pliocene to Miocene sequences were recovered during Leg 177 at Sites 1088, 1090 and 1091 (Gersonde et al., 1999). Preliminary shipboard biostrati-

graphic study showed that nannofossil assemblages are relatively well-preserved at Sites 1088 and 1090 (Shipboard Scientific Party, 1999a,b).

Although many legs have been carried out in the Southern Ocean (DSDP Leg 71, ODP Legs 113, 114, 119 and 120), no accurate Pliocene to Miocene calcareous nannofossil biostratigraphy is available for this area because of poor recovery, core disturbance, presence of hiatuses or no car-

* Corresponding author.

E-mail address: marino@geo.uniba.it (M. Marino).

bonate recovery in the late Neogene. With respect to this, Site 1088, located at $41^{\circ}8.2'S$, $13^{\circ}33.7'E$ (Fig. 1), offers an opportunity to improve the nannofossil biostratigraphy at this latitude since it seems to show a continuous middle–upper Miocene to Pliocene carbonate sequence with relatively high sedimentation rates, varying from 11 m/Myr (middle Miocene) to 17–30 m/Myr (late Miocene) and 7 m/Myr (Pliocene). Unfortunately, no geomagnetic data are available from this site (Shipboard Scientific Party, 1999a).

At Site 1090, drilled at $42^{\circ}54.8'S$, $8^{\circ}54'E$ (Fig. 1), a major hiatus at around 70 mcd (meters composite depth) separates lower Pliocene from lower to middle Miocene sequences. This is marked by a lithological change from reddish muddy nannofossil ooze to white nannofossil ooze (Shipboard Scientific Party, 1999b). As indicated by the quality of the shipboard data at this site excellent geomagnetic data will be available, which will allow a

detailed correlation between the calcareous nannofossil bioevents and the geomagnetic polarity time scale. However, at this time no shore-based geomagnetic data from the site have been published.

2. Materials and methods

One to two samples per section from cores 5H to 15H at Site 1090B and from cores 3H to 13X at Site 1088B were analyzed. Smear slides were prepared from unprocessed sediment and were examined with a light microscope (Zeiss 'Axioskop') at $\times 1000$ magnification; $\times 1600$ magnification was also used for the identification of very small specimens $< 3 \mu\text{m}$. About 2.64 mm^2 of smear slides (150 fields of view) were examined in order to estimate semi-quantitative abundance of nannofossils. Moreover, two additional traverses of

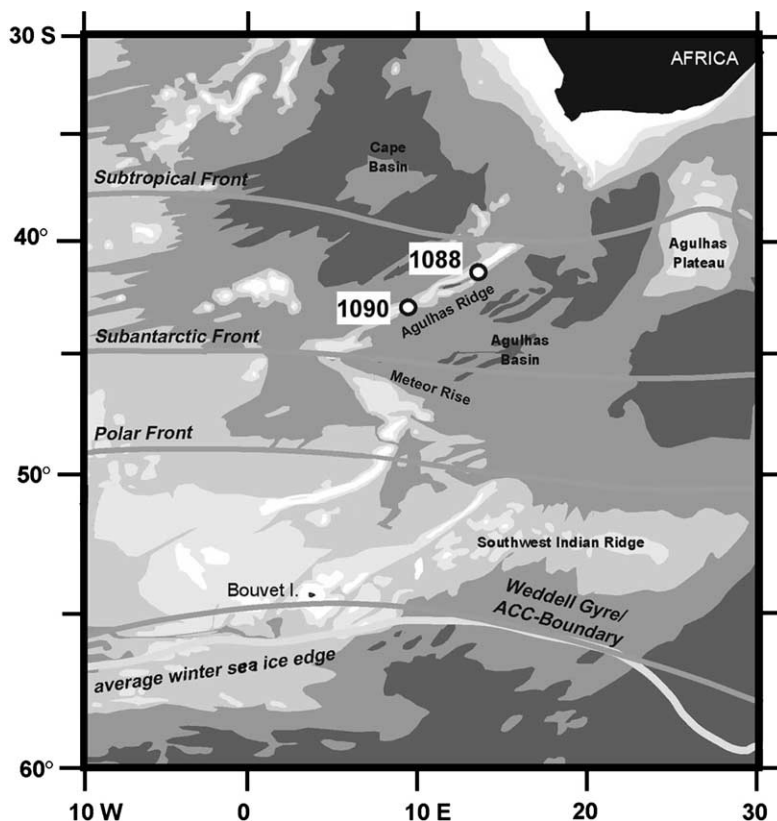


Fig. 1. Location map of Sites 1088 and 1090.

slides were scanned to recognize the presence of very rare species. Quantitative abundances of *Discoaster* spp. were determined in the Miocene–Pliocene interval by counting the number of specimens of the genus within 150 fields of view. Abundances were plotted as number of specimens per unit area of smear slide according to the counting technique of Backman and Shackleton (1983) and Rio et al. (1990a,b); these abundance patterns were considered useful to define the first and last occurrences (FO and LO) of index species. Small *Gephyrocapsa* specimens were counted within a total as 50 small coccoliths (< 5 µm) in order to show the small *Gephyrocapsa* that occurs at the lower–middle Pliocene boundary. Other genera (helicoliths, sphenoliths, ceratolithids, *Triquetrorhabdulus* spp.) useful for Miocene biostratigraphy were rare and sporadic or even absent, and prevented any quantitative analyses for more precise zonal attribution.

3. Biostratigraphic results

The zonal schemes of Martini (1971) and Okada and Bukry (1980) were adopted for Miocene and Pliocene interval at Sites 1088 and 1090. In addition, other bioevents were used to improve nannofossil biostratigraphy based on quantitative analyses of Olafsson (1989), Fornaciari et al. (1990, 1993, 1996), Rio et al. (1990a), Bukry (1991), Gartner (1992), Raffi and Flores (1995), Raffi et al. (1995), Fornaciari and Rio (1996), De Kaenel and Villa (1996), Maiorano and Monnechi (1998). Fig. 2 shows the chronostratigraphy, standard biozones, biozonal events, as well as additional events according to the literature and this work, as discussed in the text. Nannofossil range charts of Sites 1088 and 1090 are available in Marino and Flores (in press, ODP Leg 177 SR) to whom the reader may refer for more details on the abundance and distribution of calcareous nannofossils.

3.1. ODP Site 1088

3.1.1. Pliocene

The Pliocene interval is characterized by abun-

dant and generally well-preserved nannoflora thus allowing the recognition of several events (Table 1). Quantitative and semi-quantitative analyses provide reliable distribution for some markers (*Discoaster brouweri*, *D. pentaradiatus*, *D. surculus*, *D. tamalis*, *D. hamatus*, *D. quinqueramus*, *Reticulofenestra pseudoumbilicus*), the LOs of which are biozonal boundaries in the standard schemes (Figs. 2–4). The interval above 20.725 mcd is assigned to NN19 on the basis of the LO of *D. brouweri*; the bases of NN18 and NN17 were recognized on the basis of the LOs of *D. pentaradiatus* and *D. surculus* at 22.6 and 23.375 mcd, respectively (Fig. 4); the LO of *R. pseudoumbilicus* (*Reticulofenestra* > 7 µm in size) marked the base of NN16 at 33.65 mcd (Figs. 2 and 3). The LO of *Sphenolithus* spp. (*S. abies*, *S. neoabies*) occurs just above the disappearance of *R. pseudoumbilicus*, at 32.3 mcd, confirming its stratigraphic position slightly above the base of NN16. An acme of small *Gephyrocapsa* occurs between 32.3 and 36.545 mcd starting above the FO of *Pseudoemiliana lacunosa* and contemporary with the FO of *D. tamalis* (Fig. 4). The end acme of small *Gephyrocapsa* is coincident with the LO of *Sphenolithus* spp. (*S. abies* and *S. neoabies*), just above the LO of *R. pseudoumbilicus* (Fig. 3). Yet, this acme event is calibrated neither to geomagnetic scales nor to isotope stratigraphy. However, a first consistent occurrence of small *Gephyrocapsa* was reported by Samtleben (1980) within zone NN15. A similar distribution of small *Gephyrocapsa* in the upper part of the lower Pliocene is recorded at Site 1092 (Shipboard Scientific Party, 1999c) and in terrigenous sediments of the Mediterranean area (Driever, 1988; Marino, 1994). Small *Gephyrocapsa* become abundant again within the upper Pliocene and the Pleistocene, where they also show several acme events (Gartner, 1988; Rio et al., 1990b; Castradori, 1993; Raffi et al., 1993). The occurrence of small *Gephyrocapsa* acme events seems to be linked to stressed environmental conditions because these placoliths, as small *Reticulofenestra* and Pleistocene *Emiliana huxleyi*, are considered opportunistic species whose high abundance can be correlated to cold and high-fertility water (Gartner et al., 1987; Gartner, 1988, 1992). The global value of the

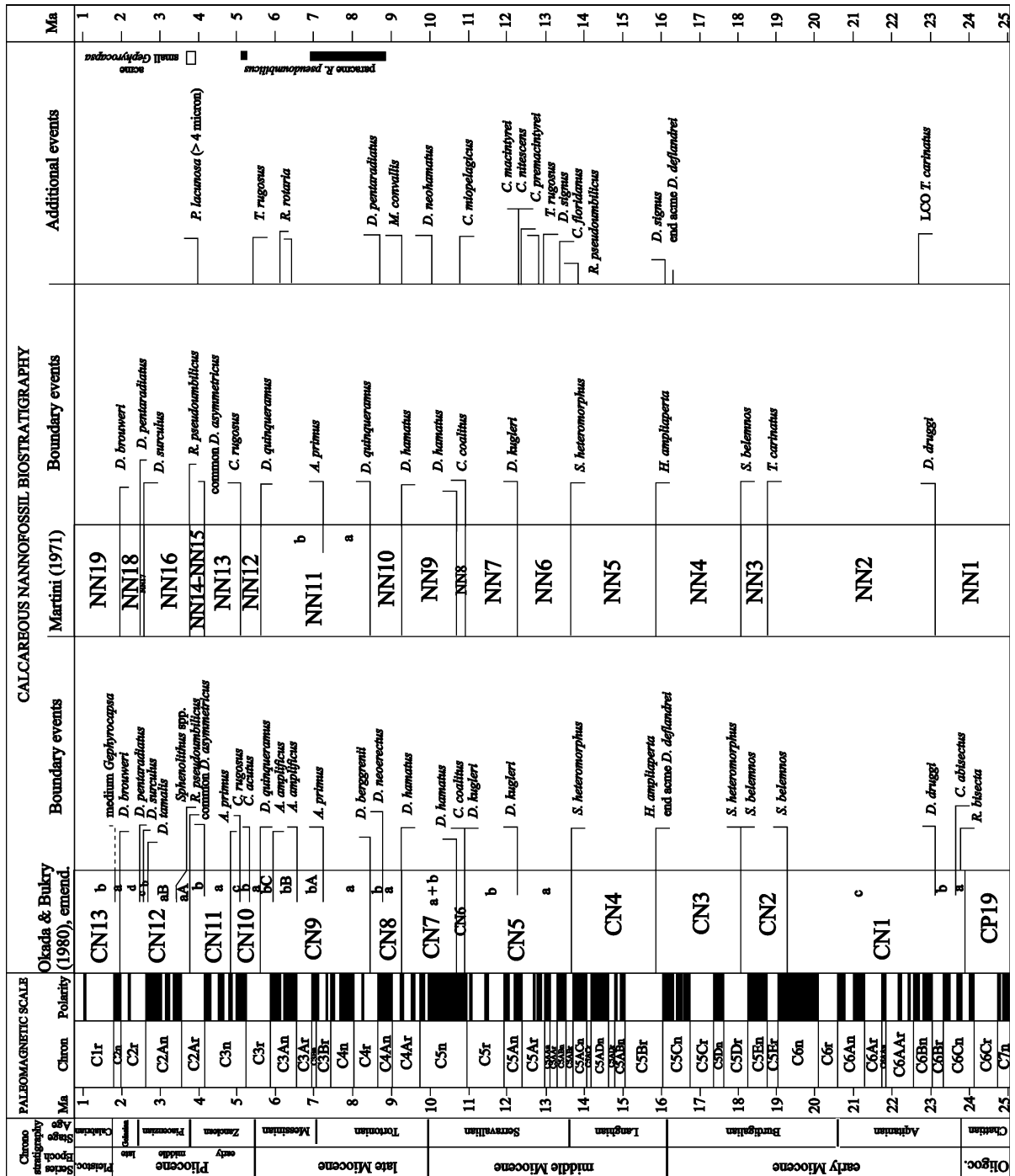


Fig. 2. Chronostratigraphy and calcareous nannofossil biostratigraphy adopted in this work. Geomagnetic polarity time scale is according to Berggren et al. (1995). The emendation of the zones CN9 and CN12 of Okada and Bukry (1980) is according to Raffi and Flores (1995) and Bukry (1991), respectively.

Table 1
Interval samples and depth of calcareous nannofossil events at Site 1088

| Nannofossil event | | Depth range of stratigraphic datums | | | | | | | | | | | | | | | | Age (Ma) | | | | |
|-------------------|---|-------------------------------------|---|----|---|------|-----|--------|--------|--------|------|------|-----|------|-----|-----|-----|-------------|--------|---------|---------|--------------------|
| | | Top | | | | | | | | Base | | | | | | | | | Mean | | | |
| | | Sample | | | | mbsf | mcd | Sample | | | | mbsf | mcd | mbsf | mcd | | | | | | | |
| LO | <i>Discoaster brouweri</i> | 1088 | B | 3 | H | 4 | 105 | 106 | 20.55 | 20.55 | 1088 | B | 3 | H | 4 | 140 | 140 | 20.9 | 20.9 | 20.725 | 20.725 | 1.95 ^a |
| LO | <i>Discoaster pentaradiatus</i> | 1088 | B | 3 | H | 5 | 140 | 140 | 22.4 | 22.4 | 1088 | B | 3 | H | 6 | 30 | 31 | 22.8 | 22.8 | 22.6 | 22.6 | 2.45 ^b |
| LO | <i>Discoaster surculus</i> | 1088 | B | 3 | H | 6 | 70 | 70 | 23.2 | 23.2 | 1088 | B | 3 | H | 6 | 105 | 106 | 23.55 | 23.55 | 23.375 | 23.375 | 2.55 ^c |
| LO | <i>Discoaster tamalis</i> | 1088 | B | 4 | H | 1 | 70 | 70 | 25.2 | 25.2 | 1088 | B | 4 | H | 1 | 140 | 140 | 25.9 | 25.9 | 25.55 | 25.55 | 2.83 ^c |
| LO | <i>Sphenolithus</i> spp. | 1088 | B | 4 | H | 5 | 140 | 140 | 31.9 | 31.9 | 1088 | B | 4 | H | 6 | 70 | 70 | 32.7 | 32.7 | 32.30 | 32.3 | 3.66 ^d |
| LO | <i>Reticulofenestra pseudoumbilicus</i> | 1088 | B | 4 | H | 6 | 140 | 140 | 33.4 | 33.4 | 1088 | B | 4 | H | 7 | 40 | 40 | 33.9 | 33.9 | 33.65 | 33.65 | 3.8 ^d |
| FO | <i>Discoaster tamalis</i> | 1088 | B | 5 | H | 2 | 70 | 70 | 36.20 | 36.20 | 1088 | B | 5 | H | 2 | 139 | 139 | 36.89 | 36.89 | 36.545 | 36.545 | |
| FO | <i>Pseudoemiliania lacunosa</i> | 1088 | B | 5 | H | 4 | 70 | 70 | 39.20 | 39.20 | 1088 | B | 5 | H | 4 | 140 | 140 | 39.90 | 39.90 | 39.55 | 39.55 | 4.00 ^e |
| FCO | <i>Discoaster asymmetricus</i> | 1088 | B | 5 | H | 4 | 140 | 140 | 39.9 | 39.9 | 1088 | B | 5 | H | 5 | 68 | 68 | 40.68 | 40.68 | 40.29 | 40.29 | |
| LO | <i>Discoaster quinqueramus</i> | 1088 | B | 6 | H | 5 | 70 | 70 | 50.2 | 50.2 | 1088 | B | 6 | H | 7 | 12 | 12 | 52.6 | 52.6 | 51.4 | 51.4 | 5.54 ^f |
| FO | <i>Amaurolithus</i> spp. | 1088 | B | 8 | H | 6 | 130 | 130 | 71.2 | 71.2 | 1088 | B | 8 | H | CC | 10 | 15 | 71.37 | 71.37 | 71.29 | 71.285 | 7.39 ^f |
| FO | <i>Discoaster quinqueramus</i> | 1088 | B | 11 | H | 4 | 130 | 130 | 96.8 | 96.8 | 1088 | B | 11 | H | 5 | 70 | 70 | 97.7 | 97.7 | 97.25 | 97.25 | 8.6 ^g |
| LO | <i>Discoaster hamatus</i> | 1088 | B | 13 | H | 1 | 70 | 70 | 110.7 | 110.7 | 1088 | B | 13 | H | 3 | 70 | 70 | 113.7 | 113.7 | 112.2 | 112.2 | 9.63 ^f |
| FO | <i>Discoaster hamatus</i> | 1088 | C | 4 | H | 1 | 70 | 70 | 144 | 142.14 | 1088 | C | 4 | H | 1 | 140 | 140 | 144.7 | 142.84 | 144.35 | 142.49 | 10.47 ^f |
| LO | <i>Coccolithus miopelagicus</i> | 1088 | C | 7 | X | 4 | 140 | 140 | 171.57 | 169.71 | 1088 | C | 7 | X | CC | 16 | 21 | 171.83 | 169.97 | 171.70 | 169.84 | 10.94 ^f |
| FO | <i>Calcidiscus macintyreii</i> | 1088 | C | 11 | X | 4 | 20 | 21 | 208.57 | 206.49 | 1088 | C | 11 | X | CC | 72 | 77 | 209.37 | 207.29 | 208.97 | 206.89 | 12.34 ^d |
| LO | <i>Calcidiscus premacintyreii</i> | 1088 | C | 11 | X | 4 | 20 | 21 | 208.57 | 206.49 | 1088 | C | 11 | X | CC | 72 | 77 | 209.37 | 207.29 | 208.97 | 206.89 | 12.65 ^d |
| LCO | <i>Cyclicargolithus floridanus</i> | 1088 | C | 12 | X | 1 | 20 | 20 | 214.30 | 212.44 | 1088 | C | 12 | X | CC | 89 | 94 | 215.37 | 213.51 | 214.835 | 212.975 | 13.2 ^d |

^a Raffi et al. (1993).

^b Lourens et al. (1996).

^c Thiedemann et al. (1994).

^d Raffi and Flores (1995).

^e Gartner (1990).

^f Backman and Raffi (1997).

^g Berggren et al. (1995).

Pliocene acme of small *Gephyrocapsa* requires further investigation on many sites because its occurrence could have both paleoceanographic and stratigraphic significance.

Biozonal events between the LO of *Reticulofenestra pseudoumbilicus* and the LO of *Discoaster quinqueramus* were not recognized for a reliable attribution to the zones NN13 and NN14–15, due to the absence of *Ceratolithus rugosus* and the rarity of *Discoaster asymmetricus*. However, the first common occurrence (FCO) of *D. asymmetricus* is tentatively placed at 40.29 mcd where the presence of the species becomes almost continuous in the Pliocene record (Fig. 4), thus inferring a possible base of NN14–15 at this depth. Consequently, the interval from 33.65 to 40.29 mcd and the interval from 40.45 to 51.4 mcd were referred to NN12–13 and NN14–15 combined zones (Fig. 3). The first occurrences of *Discoaster tamalis* and *Pseudoemiliana lacunosa* (> 4 µm) have been recorded at 36.545 mcd and 39.55 mcd, respectively. These events are known to fall within the zones NN14–15 according to Rio et al. (1990b) and Gartner (1990). Samtleben (1980) reports the FO of *P. lacunosa* as occurring within the NN15 zone. The age assignment for the FO of *P. lacunosa* is around 4.0 Ma (Gartner, 1990), but a well-calibrated biochronology of the event is not supported by enough data from Pliocene literature of many geographic areas. Although no geomagnetic data are available at Site 1088 for the calibration of the FO of *P. lacunosa* this event may be considered reliable for approximating the base of NN15 when classical zonal marker species are absent. An unambiguous taxonomic criterion and quantitative abundance pattern of the species in well-preserved material are necessary to define exactly this event. In fact, *P. lacunosa* is also characterized by elliptical and small specimens (< 4 µm) close to its first appearance and may be confused with small reticulofenestrids in poorly preserved nannofossil assemblages. According to Fornaciari (1996), the FCO may rep-

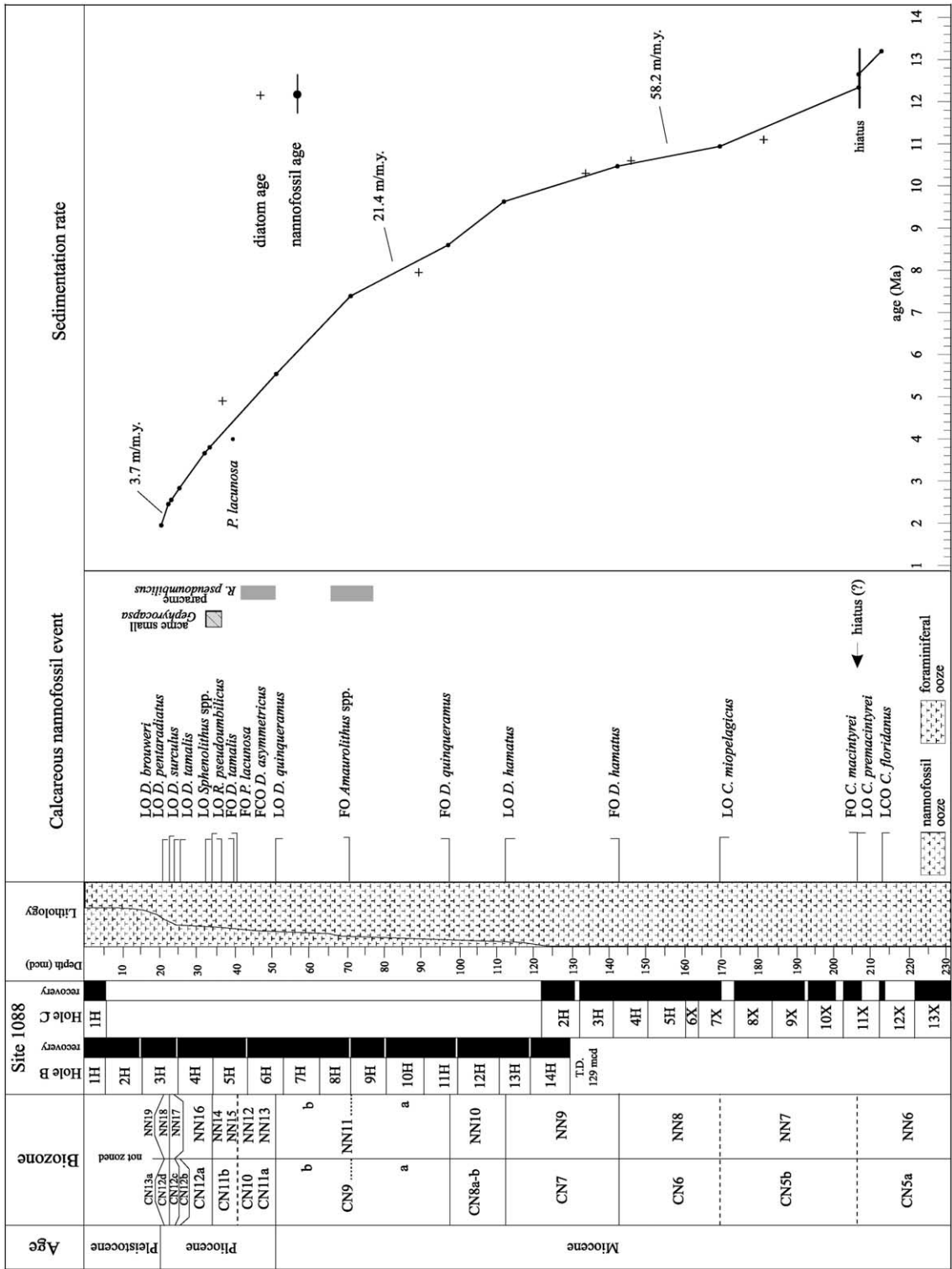
resent a more reliable biostratigraphic event to indicate a significant entrance of *P. lacunosa* in the Pliocene nannofossil assemblages. The FCO of *P. lacunosa* at Site 1088 might be placed at 36.545 mcd between the FCO of *D. asymmetricus* and the LO of *R. pseudoumbilicus*, in agreement with quantitative data of Fornaciari (1996).

At the base of the interval referred to the Pliocene NN12–NN13 combined zones it is worth noting the absence or rarity of *Reticulofenestra pseudoumbilicus* (> 7 µm) (Fig. 5). A Pliocene paracme of the species is known to occur between 5.01 and 5.2 Ma (Di Stefano et al., 1996) in the Mediterranean area (Rio et al., 1990b; Di Stefano et al., 1996). Semi-quantitative data on reticulofenestrids at Site 1088 (Marino and Flores, in press, ODP SR) seem to be in good agreement with the *R. pseudoumbilicus* paracme occurring in the Mediterranean area.

3.1.2. Miocene

Because taxa of the genera *Ceratolithus* and *Triquetrorhabdulus* are absent at Site 1088, the Miocene/Pliocene boundary could not be defined based on the FO of *C. acutus* and the LO of *Triquetrorhabdulus rugosus*. However, the LO of *Discoaster quinqueramus* that approximates the Miocene/Pliocene boundary according to Backman and Raffi (1997) and defines the base of NN12 was recognized at 51.5 mcd (Table 1, Figs. 2 and 3). The first rare presence of *Amaurolithus primus* was identified at 71.258 mcd. Although the genus is very poorly represented at Site 1088 the base of NN11b is tentatively placed between samples 177-1088B-8H-6, 130 cm and 177-1088B-8H-CC (Fig. 3). A temporary absence of *Reticulofenestra pseudoumbilicus* is recorded at this level, from about 65.4 to 77.2 mcd, which is from below to above the base of NN11b (Figs. 3 and 5). The Miocene paracme of *Reticulofenestra* > 7 µm (*R. pseudoumbilicus* > 7 µm) is reported in the literature (Pujos, 1987; Young, 1990, 1998; Rio et al., 1990a; Young et al., 1994; Raffi and

Fig. 3. Chronostratigraphy, biostratigraphy and sedimentation rate at Site 1088. The diatom age points are (from top to bottom): FOD *Thalassiosira inura*, FOD *Fragilariopsis reinholdii*, FOD *Asteromphalus kennettii*, LOD (last occurrence datum) *Deniculopsis ovata*, FOD *D. ovata*.



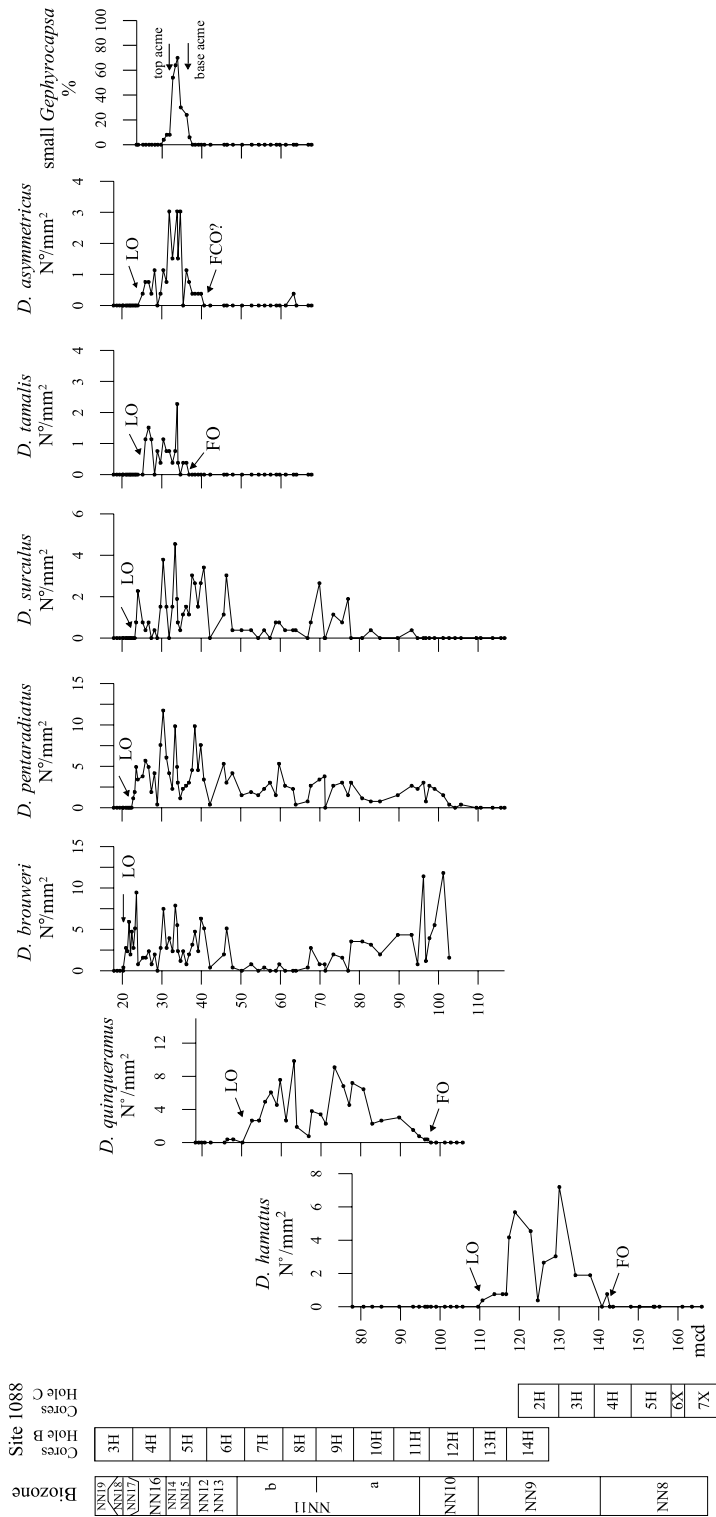


Fig. 4. Abundance pattern of selected Miocene-Pliocene marker species at Site 1088.

Flores, 1995; Raffi et al., 1995) as occurring from the base of NN10b to above the NN11a/NN11b boundary (Young, 1990, 1998; Young et al., 1994). This datum seems to be widely isochronous (Young et al., 1994) and corresponds to an interval characterized by abundant small reticulofenestrids < 3 μm in size (Young, 1998), which also have been found at abundant and very abundant occurrences, together with reticulofenestrids 3–5 μm in size, in the upper Miocene nannofossil assemblages of Site 1088. The semi-quantitative analyses on the reticulofenestrid complex of Site 1088 show a more continuous dominance of specimens < 5 μm within the paracme of *Reticu-*

lofenestra > 7 μm, whereas specimens > 5 μm are dominant in the NN6–NN11a biozonal interval. This pattern is in accordance with data presented by Young (1998). Despite the fact that our semi-quantitative data are not accurate enough to be compared in detail to quantitative data presented by Young (1990) and Takayama (1993), the distribution patterns of *Reticulofenestra* spp. obtained at Site 1088 (Fig. 5) show close affinities with the quantitative records. Exception is the slightly younger beginning of the Miocene paracme of *R. pseudoumbilicus* > 7 μm at Site 1088.

The base of NN11a (Fig. 3) is defined on the basis of the FO of *Discoaster quinquerramus* at

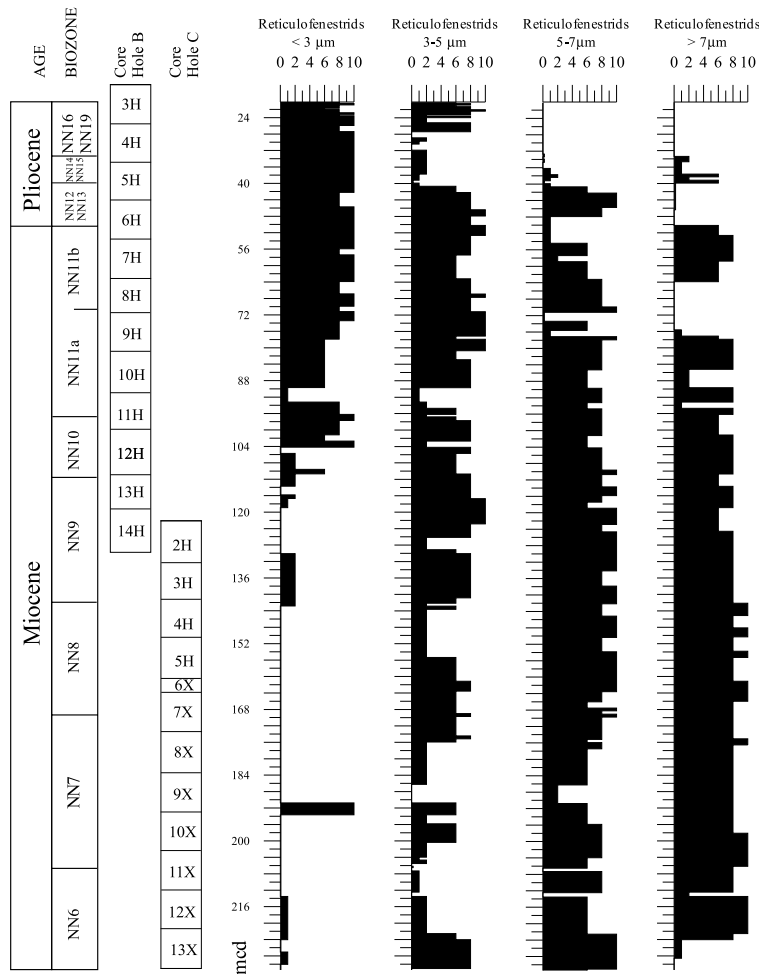


Fig. 5. Distribution of reticulofenestrids at Site 1088. The abundance scale is a numerical representation of semi-quantitative abundance values: 0 = absent, 0.2 = very rare, 1 = rare, 2 = few, 6 = common, 8 = abundant, 10 = very abundant.

97.25 mcd. The first rare and scattered presence of *Discoaster surculus* is recorded within this biozone (Fig. 4). The LO of *Discoaster hamatus* occurs at 112.2 mcd and defines the base of NN10 (Figs. 3 and 4). The distribution of *D. hamatus*, even if rare specimens represent the species, is almost continuous and the FO of the species is recorded at 142.49 mcd allowing the recognition of the base of NN9.

The species *Catinaster coalitus* and *Discoaster kugleri* are not recorded at Site 1088, which prevents a standard definition of the bases of the NN8 and NN7 zones. However, additional events are reported in the literature close to these zonal boundaries. We used the LO of *Coccolithus miopelagicus* (at 169.84 mcd) and the FO of *Calcidiscus macintyreii* (at 206.89 mcd) to roughly approximate the NN7/NN8 boundary and the base of NN7 (Figs. 2 and 3), respectively.

The LO of *Calcidiscus premacintyreii* occurs at 206.89 mcd together with the FO of *Calcidiscus macintyreii* ($> 11 \mu\text{m}$). Considering that the two events are dated at 12.65 and 12.34 Ma (Shackleton et al., 1995), respectively, their co-occurrence suggests the presence of a short hiatus at this depth (Fig. 3).

Cyclicargolithus floridanus has its LO at 212.975 mcd. The event falls within the lower CN5 zone (Bukry, 1973; Raffi et al., 1995; Maiorano and Monechi, 1998) and occurs above the LO of *Sphenolithus heteromorphus* and the FO of *Reticulofenestra pseudoumbilicus*. The absence of *S. heteromorphus* and the presence of common *R. pseudoumbilicus* in the lowermost portion of the sequence recovered at Site 1088 suggest that the basal sediments at Site 1088 are in zone NN6 (Fig. 3).

3.1.3. Sedimentation rates

An age–depth curve is constructed by using nannofossil (this work) and diatom (Shipboard Scientific Party, 1999a) events (Fig. 3). The ages of nannofossil events are from the literature (Table 1). There is a general agreement between nannofossil and diatom age points (Fig. 3), with exception of the FOD (first occurrence datum) of *Thalassiosira inura* at 4.92 Ma and the FO of *Pseudoemiliania lacunosa* at 4 Ma. The FOD of

T. inura should be considered unreliable because of poorly preserved diatom assemblages (Censarek and Gersonde, this issue). However, the FO of *P. lacunosa* needs to be calibrated to the GPTS by using a precise morphometric criterion ($> 4 \mu\text{m}$) in order to confirm its age assignment. The sedimentation rate obtained from the age model varies largely through time. The lowest rate, 3.75 m/Myr, was calculated for the late Pliocene, while the rate ranges between 13.6 and 21.4 m/Myr in the late Miocene, and reaches up to 58.2 m/Myr in the late middle Miocene (Fig. 3). A possible hiatus at 206.89 mcd is shown by the co-occurrence of the LO *Calcidiscus premacintyreii* and the FO of *Calcidiscus macintyreii*. However, to definitely document the occurrence of this disconformity quantitative analyses must be performed in order to exclude the possibility that the specimens of *C. premacintyreii* recorded in its uppermost range are reworked. Moreover, the FO of *C. macintyreii* is not considered a reliable event for global correlation because the marker seems to be controlled by biogeographic factors and taxonomic ambiguities might affect the accurate determination of its stratigraphic range (see discussion in Raffi et al., 1995).

3.2. ODP Hole 1090B

3.2.1. Pliocene

The Pliocene interval is characterized by abundant nannofossil assemblages with low species diversity. Nannofossil events are reported in Table 2 and Fig. 6. *Discoasters* are very poorly represented; the number of specimens of *Discoaster pentaradiatus* and *Discoaster brouweri* varies from 1 to 16 within a scanned area of 2.64 mm² (Fig. 7). Despite the rarity of these species the distribution of *D. pentaradiatus* and *Discoaster brouweri* was tentatively utilized for the recognition of the base of NN18 and NN19, respectively. *Discoaster tamalis*, *Discoaster asymmetricus* and *Discoaster surculus* were just recognized in three samples and are represented by rare (1 to 4) and scattered specimens, which prevents the recognition of the biozones NN16 and NN17. An expanded interval below the LO of *D. pentaradiatus*, between 52.85 mcd and 71 mcd, is referred to the

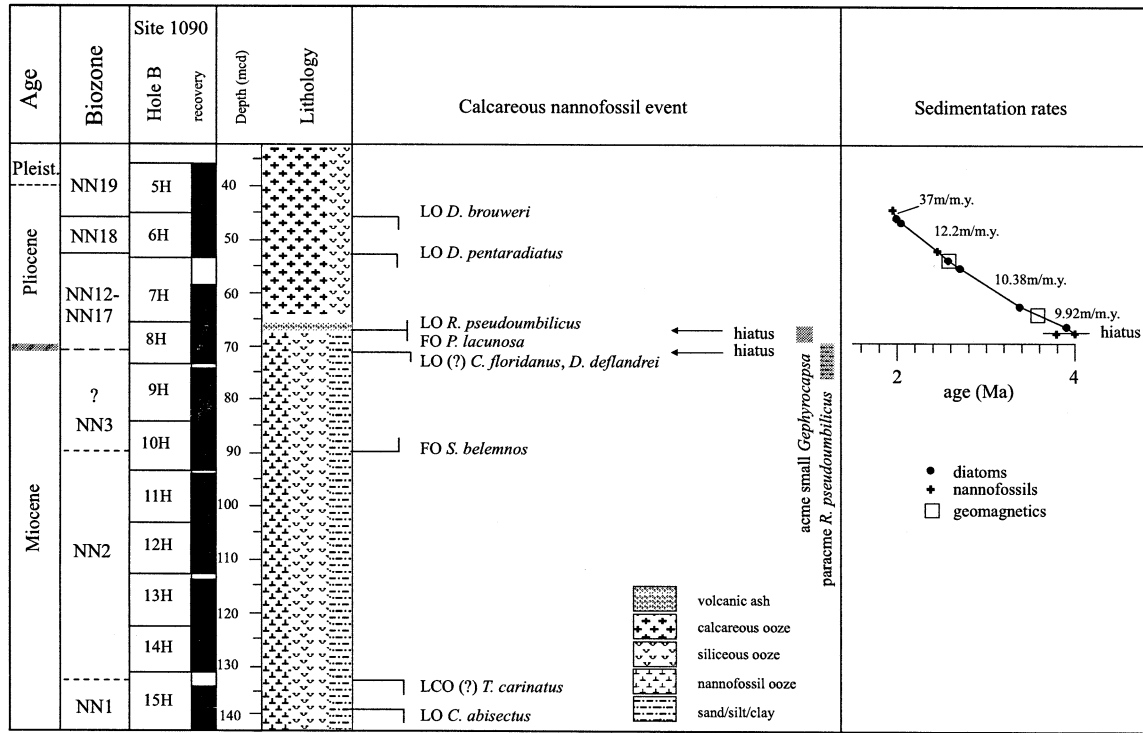


Fig. 6. Chronostratigraphy, biostratigraphy and sedimentation rate at Site 1090. The diatom age points are (from top to bottom): LOD *Thalassiosira kolbei*, LOD *Fragilariopsis matuyamae*, LOD *Thalassiosira vulnifica*, LOD *Thalassiosira insigna*, FOD *Fragilariopsis weaveri*, FOD *Fragilariopsis interfrigidaria*. The magnetic age points are (from top to bottom): top of C2An.1n and bottom of C2An.3n.

Pliocene NN12–17 combined zones since the conventional events that define the zonal boundaries of this interval (LO of *Discoaster quinquerramus*, FO of *Ceratolithus rugosus*, FO of *D. asymmetricus*, LO of *Amaurolithus tricorniculatus*, LO of *Reticulofenestra pseudoumbilicus*) were not recog-

nized. The co-occurrence of the LO of *R. pseudoumbilicus* and the FO of *Pseudoemiliana lacunosa* ($> 4 \mu\text{m}$) whose age assignments are 3.8 Ma (Shackleton et al., 1995) and 4.0 Ma (Gartner, 1990), respectively, suggests the occurrence of a disconformity in the interval between 66.71 and

Table 2
Interval samples and depth of calcareous nannofossil events at Site 1090

| Event | Sample interval | mcd | mbsf | Remarks | Age (Ma) |
|--|-----------------------|-------|-------|---------|-------------------|
| LO <i>Reticulofenestra pseudoumbilicus</i> | 8 H-2, 30/8 H-2, 140 | 67.26 | 63.55 | hiatus | 3.8 ^a |
| FO <i>Pseudoemiliana lacunosa</i> | 8 H-2, 30/8 H-2, 140 | 67.26 | 63.55 | hiatus | 4.0 ^b |
| LO <i>Discoaster pentaradiatus</i> | 6 H-6, 130/6 H-7, 30 | 52.85 | 51.25 | | 2.45 ^c |
| LO <i>Discoaster brouweri</i> | 6 H-1, 130/6 H-2, 130 | 45.85 | 44.25 | | 1.95 ^d |

^a Raffi and Flores (1995).

^b Gartner (1990).

^c Lourens et al. (1996).

^d Raffi et al. (1993).

67.81 mcd (between samples 177-1090B-8H-2, 30 cm, and 177-1090B-8H-2, 140 cm). Around this disconformity (from sample 177-1090B-8H-1, 120 cm at 66.11 mcd to sample 177-1090B-8H-3, 30 cm at 68.21 mcd) we mark the common occurrence of very small *Gephyrocapsa* ($< 3.5 \mu\text{m}$ in size) (Fig. 7). As discussed above (see 3.1. ODP Site 1088), these placoliths seem to characterize the Pliocene interval ranging from close to the FO of *P. lacunosa* to close to the LO of *R. pseudoubilicus*. A short interval, characterized by the absence of *R. pseudoubilicus*, occurs at the base of the inferred Pliocene interval, from sample 177-1090B-8H-4, 30 cm (69.71 mcd), to sample 177-1090B-8H-4, 139 cm (70.8 mcd). A paracme of this species is recorded in the lower Pliocene of the Mediterranean area (Rio et al., 1990a,b; Di Stefano et al., 1996) between 5.2 and 5.01 Ma (Di Stefano et al., 1996) and at a correlative level of Site 1088. We cannot confirm the stratigraphic value of this paracme because the lower Pliocene nanoflora is not diagnostic of precise interval time at Site 1090. Nevertheless, the short absence of *R. pseudoubilicus* from sample 177-1090B-8H-4, 139, to sample 177-1090B-8H-4, 30, could indicate the presence of the NN12 zone. The same interval is characterized by the presence of abundant to dominant small reticulofenestrids ($< 3 \mu\text{m}$ and $3\text{--}5 \mu\text{m}$ in size) including specimens referable

to small *Dictyococcites* ($< 5 \mu\text{m}$), which characterize lower Pliocene assemblages according to Backman (1980). This interpretation is consistent with foraminiferal data of Galeotti et al. (this issue). The latter authors place the base of Pliocene at 71.5 mcd, based on the FO of *Globorotalia puncticulata* and *Globorotalia crassaformis*.

3.2.2. Miocene

The calcareous nannofossil record is marked by a distinct change in nannofossil assemblage composition between samples 177-1090B-8H-4, 139 cm, and 177-1090B-8H-5, 30, at 71.0 mcd. While typical lower and middle Miocene taxa such as *Cyclicargolithus floridanus* and *Discoaster deflandrei* abruptly disappear, small *Dictyococcites* and small *Reticulofenestra* ($< 5 \mu\text{m}$) become dominant or abundant just above 71.0 mcd. This change marks a disconformity between the Miocene and Pliocene sequences. However, the establishment of a detailed calcareous nannofossil-based biostratigraphic zonation of the Miocene sequences from Site 1090 (interval from sample 177-1090B-8H-5, 30 cm, to sample 177-1090B-15H-CC) is impeded by the low and discontinuous occurrence of marker species, the generally poor to very poor preservation of the calcareous nannofossils and possible reworking.

The assemblages encountered between samples

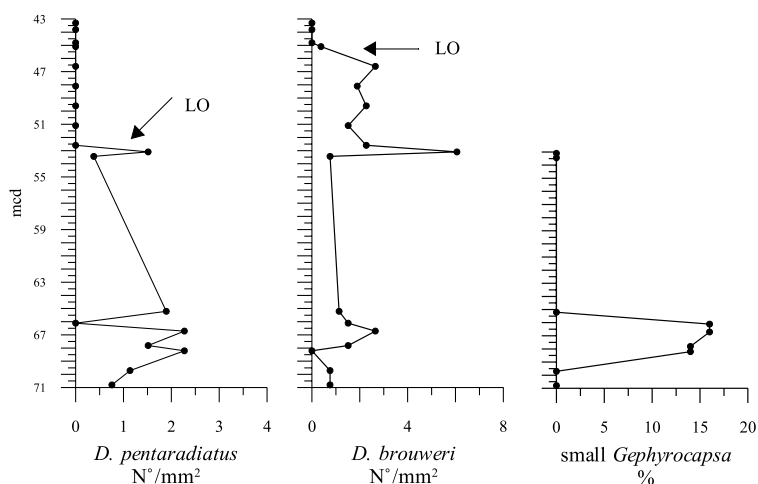


Fig. 7. Abundance pattern of selected Pliocene marker species at Site 1090.

8H-5, 30 cm (71.21 mcd), and 9H-6, 30 cm (82.19 mcd) are dominated by *Coccolithus pelagicus*, *Discoaster deflandrei* and *Cyclicargolithus floridanus*. The presence of *Reticulofenestra pseudumbilicus*, which has its FO in the uppermost portion of the middle Miocene NN5 zone, and the absence of *Sphenolithus heteromorphus*, whose LO marks the boundary between NN5 and NN6 (Fig. 2), may indicate that these sediments have been deposited after the middle middle Miocene. The lack of *R. pseudumbilicus* in assemblages encountered between 71.21 and about 73.34 mcd probably indicates that this interval correlates with the *R. pseudumbilicus* paracme, which occurs in the upper Miocene NN10–NN11a zones according to Young (1998). This interpretation is supported by the occurrence in a sample at 72.31 mcd (see range chart in Marino and Flores, in press, ODP SR) of one poorly preserved specimen referable to the *Minylitha convallis* taxon, which has its FO in the late Miocene (Fig. 2). Such interpretation of the interval between 82 and 71 mcd would indicate that this section is strongly disturbed by reworking of stratigraphically older calcareous nanofossils, such as *C. floridanus* and *D. deflandrei*, and possible disconformities. The last common occurrences (LCOs) of the latter two taxa fall within the lower NN6 and NN4, respectively (Bukry, 1973; Raffi et al., 1995; Maiorano and Monechi, 1998; Young, 1998).

Divergent of the latter age model for the interval between 71.21 and 82.19 mcd is a stratigraphic interpretation, which is based on the assumption that the common to abundant presence of both *Discoaster deflandrei* and *Cyclicargolithus floridanus* represents an autochthonous occurrence. Considering that the LCO of *D. deflandrei* is in the late lower Miocene NN4 zone, such interpretation would indicate that the interval below the hiatus at around 71 mcd is not younger than early Miocene. The absence of *Sphenolithus heteromorphus*, which ranges within the lower Miocene and early middle Miocene NN4 and NN5 zones, might further show that the sequence is older than the NN4. However, at Site 1090 also other Miocene marker taxa, such as *Sphenolithus belemnus* and *Discoaster druggi*, occur very rarely (few specimens of *S. belemnus* between 89.17 and 86.17

mcd) or were not found, respectively. This pattern might indicate the general absence or scarceness of some of the middle and lower Miocene stratigraphic marker species from the area of investigation, due to the poor preservation or paleoceanographic reasons. In fact, a latest early Miocene age within the geomagnetic chron C5Cn has also been proposed by Billups et al. (in press) for the sequences immediately below the hiatus at around 71 mcd, based on an age model established by combining isotope and geomagnetic records. The age model of Billups et al. (in press) is also consistent with the rare occurrence of *S. belemnus*, because the interval between 89.17 and 86.17 mcd was interpreted to fall within chron C5En, which is in the stratigraphic range of the taxon, the NN3 zone (Fig. 3). Following this model, the FO of *Reticulofenestra pseudumbilicus* should be placed in the early Miocene, in agreement with the distribution of the species shown by De Kanel and Villa (1996) in some ODP sites from north-eastern Atlantic Ocean.

The interval from samples 177-1090B-10H-4, 130 (90.57 mcd) cm, to 177-1090B-15H-CC (143.22 mcd) is interpreted to be in the upper Oligocene to lower Miocene zones NN1–NN2. Because of the absence of *D. druggi*, whose FO marks the base of zone NN2, we propose to approximate the base of the NN2 zone using the LCO of *Triquetrorhabdulus carinatus*, encountered between samples 177-1090B-14H-CC, 0–5 cm (127.51 mcd), and 15H-1, 30 cm (134.49 mcd). The LCO of this species, which however occurs at Site 1090 only rarely, is considered a reliable event at the base of CN1c (Rio et al., 1990a; Gartner, 1992; Fornaciari et al., 1993; Maiorano and Monechi, 1998), which falls in the upper part of geomagnetic chron C6Bn (Gartner, 1992; Maiorano and Monechi, 1998). This is in close accordance with the interpretation of the geomagnetic polarity record proposed by Billups et al. (in press), which indicates that the interval from 134.39 to 127.51 mcd correlates with chrons C6Br and C6Bn, close to the occurrence of the Mil.1 oxygen isotope event, recognized at 133.84 mcd. *Cyclicargolithus abisectus* was encountered in the lower part of the Miocene section at Site 1090. The LO of the taxon could be

placed at 138.75 mcd. According to Okada and Bukry (1980) the LO of the species defines the base of CN1b, which correlates with the middle portion of chron C6Cn and thus represents a datum close to the Oligocene/Miocene boundary. Such age interpretation for interval with the LO of *C. abisectus* is in close accordance with the age interpretation proposed by Billups et al. (in press), who place the core depth around 138.75 mcd in chron C6Cn.

3.2.3. Sedimentation rate

At Site 1090 we only propose an age–depth model for the Pliocene sequences, based on a combination of our calcareous nannofossil stratigraphic interpretation and shipboard diatom and geomagnetic age points (Shipboard Scientific Party, 1999b; Channell and Stoner, personal communication) (Fig. 6). In the absence of shore-based geomagnetic data for the Miocene interval of Site 1090 and due to the low number of well-defined age points based on our calcareous nannofossil stratigraphy, which prevents a detailed stratigraphic interpretation of the shipboard geomagnetic polarity record, the establishment of a well-defined age–depth relationship of the Miocene section of Site 1090 is not possible using solely calcareous nannofossil stratigraphic data. Concerning the Pliocene age interpretation, no major discrepancies occur between nannofossil age assignments and diatom interpolated ages. Both the nannofossil and diatom ages fit well with the geomagnetic age points. The sedimentation rate ranges between 37 m/Myr in the late late Pliocene and 12.2 m/Myr and 10.38–9.92 m/Myr in the early late and the early Pliocene, respectively. A hiatus spanning ca. 0.2 Myr is evident at 66.76 mcd as indicated by the co-occurrence of the LO of *Reticulofenestra pseudoumbilicus* and the FO of *Pseudoemiliana lacunosa*.

4. Summary

The schemes of Martini (1971) and Okada and Bukry (1980) were used for the recognition of zonal boundaries in the Miocene and Pliocene intervals at Sites 1088 and 1090. The occurrence

of taxa belonging to *Discoaster* in the late Miocene and especially in the middle and late Pliocene was useful to recognize nannofossil biozones at Site 1088. However, specimens of *Amaurolithus*, *Discoaster*, *Triquetrorhabdulus*, *Ceratolithus* were encountered only rarely and scattered in the lower Pliocene sequences, which impeded the determination of zonal boundaries between NN12 and NN13 at Site 1088 and between NN12 and NN17 at Site 1090. The FO of *Pseudoemiliana lacunosa* ($>4\ \mu\text{m}$) just below the LO of *Reticulofenestra pseudoumbilicus* may represent a useful event to approximate the base of NN15 in the early Pliocene age. An acme of small *Gephyrocapsa* was recorded close to the lower/middle Pliocene boundary, between the FO of *P. lacunosa* and the LOs of *R. pseudoumbilicus* and *Sphenolithus* spp. Few data are available in the literature about this acme, which might be of biostratigraphic and paleoceanographic interest. However, both, the acme of small *Gephyrocapsa* and the FO of *P. lacunosa*, require further investigation and calibration to the geomagnetic polarity time scale to improve the nannofossil biostratigraphic zonation of the early Pliocene in southern high latitudes. A paracme of *R. pseudoumbilicus* occurs at both sites, 1088 and 1090, at the base of Pliocene and is similar to the temporary absence of the species known in the Mediterranean area (Rio et al., 1990b; Di Stefano et al., 1996).

An upper Miocene paracme of *Reticulofenestra pseudoumbilicus* found at Site 1088 and probably also at Site 1090 may be comparable to the paracme of the *Reticulofenestra* $>7\ \mu\text{m}$ in size reported by Young (1998, and references therein) from the zones NN10 to NN11a. However, in southern high latitudes the onset of the paracme is slightly later (top NN11a) than in middle–low-latitude areas. For further verification quantitative analyses of southern high-latitude nannofossil assemblages must be accomplished and the age models for the studied intervals must be improved. No marker species were recorded to define the NN6/NN7 and the NN7/NN8 zonal boundaries. Only the FO of *Calcidiscus macintyreii* and the LO of *Coccolithus miopelagicus* were recorded in the middle Miocene of Site 1088 and they were used to approximate the base of NN7

and the base of NN8, respectively, though these events are not considered synchronous at the global scale.

Poor preservation and low species diversity prevented the erection of a well-established age assignment for the lower Pliocene and the Miocene sequences recovered at Site 1090. Several hiatuses were inferred based on the distribution of nannofossils. While the few nannofossil datums in the lower portion of the Miocene section of Site 1090 are in agreement with an age model including geomagnetic data proposed by Billups et al. (in press), the sequence 10 m thick recovered below a Miocene/Pliocene disconformity at 71 mcd may be dated in different directions, based on the calcareous nannofossil record. One model places the sequences between 71 and 82 mcd within the middle and late Miocene and requires that most of the calcareous nannofossils preserved in this interval be reworked from older sediments. The second model, which is in agreement with the age assignment proposed by Billups et al. (in press), places the interval in the early Miocene.

Acknowledgements

We are grateful to J. Young and P. Bown for the helpful and critical revision of the manuscript. Special thanks go to R. Gersonde and N. Ciaranfi for encouragement and suggestions. Financial support for this study was provided by M.U.R.S.T. Grant 40% (1999) to N. Ciaranfi.

Taxonomic appendix

Calcareous nannofossils considered in this study are listed by alphabetical order of generic epithet. Bibliographic references for most of taxa can be found in Perch-Nielsen (1985). Any references not cited therein are included in the bibliography. Biometric definitions on problematic species adopted in this study are also reported.

Amaurolithus amplificus (Bukry and Percival, 1971) Gartner and Bukry, 1975

Amaurolithus delicatus Gartner and Bukry, 1975

Amaurolithus primus (Bukry and Percival, 1971) Gartner and Bukry, 1975

Ceratolithus tricorniculatus (Gartner, 1967) Gartner and Bukry, 1975

Calcidiscus macintyreii (Bukry and Bramlette, 1969) Loeblich and Tappan, 1978 ($\geq 11 \mu\text{m}$)

Calcidiscus premacintyreii Theodoridis, 1984

Catinaster coalitus Martini and Bramlette, 1963

Ceratolithus acutus Gartner and Bukry, 1974

Coccolithus miopelagicus Bukry, 1971 ($> 13 \mu\text{m}$)

Coccolithus pelagicus (Wallich, 1877) Schiller, 1930 ($< 13 \mu\text{m}$)

Cyclicargolithus abisectus (Müller, 1970) Wise, 1973 ($> 10 \mu\text{m}$)

Cyclicargolithus floridanus (Roth and Hay in Hay et al., 1967) Bukry, 1971 ($< 10 \mu\text{m}$)

Dietyococcites productus (Kamptner, 1963) Backman, 1980

Discoaster asymmetricus Gartner, 1969

Discoaster brouweri (Tan, 1927) emend. Bramlette and Riedel, 1954

Discoaster deflandrei Bramlette and Riedel, 1954

Discoaster druggii Bramlette and Wilcoxon, 1967 ($> 15 \mu\text{m}$)

Discoaster hamatus Martini and Bramlette, 1963

Discoaster kugleri Martini and Bramlette, 1963

Discoaster pentaradiatus (Tan, 1927) emend. Bramlette and Riedel, 1954

Discoaster quinquerramus Gartner, 1969

Discoaster signus Bukry, 1971

Discoaster surculus Martini and Bramlette, 1963

Discoaster tamalis Kamptner, 1967

Gephyrocapsa small ($< 3.5 \mu\text{m}$) sensu Gartner, 1969

Helicosphaera ampliapertura Bramlette and Wilcoxon, 1967

Pseudoemiliana lacunosa (Kamptner, 1963) Gartner, 1969, $> 4 \mu\text{m}$

Reticulofenestra bisecta (Hay, Mohler and Wade, 1967) Roth, 1970

Reticulofenestra minuta Roth, 1970 ($< 3 \mu\text{m}$)

Reticulofenestra minutula (Gartner, 1967) Haq and Berggren, 1978 (3–5 μm)

Reticulofenestra pseudoumbilicus (Gartner, 1967) Gartner, 1969 ($> 7 \mu\text{m}$)

Reticulofenestra pseudoumbilicus small (5–7 μm)

- Reticulofenestra rotaria* Theodoridis, 1984
Sphenolithus abies Deflandre in Deflandre and Fert, 1954
Sphenolithus abies/neoabies (sensu Rio et al., 1990b)
Sphenolithus belemnus Bramlette and Wilcoxon, 1967
Sphenolithus disbelemnus Fornaciari and Rio, 1996
Sphenolithus dissimilis Bukry and Percival, 1971
Sphenolithus heteromorphus Deflandre, 1953
Triquetrorhabdulus carinatus Martini, 1965
Triquetrorhabdulus rugosus Bramlette and Wilcoxon, 1967

References

- Backman, J., 1980. Miocene–Pliocene nannofossils and sedimentation rates in the Hatton-Rockall Basin, NE Atlantic Ocean. *Acta Univ. Stockholm Stockholm Contrib. Geol.* 36, 1–91.
- Backman, J., Raffi, I., 1997. Calibration of Miocene events to orbitally tuned cyclostratigraphies from Cera Rise. In: Shackleton, N.J., Curry, W.B., Richter, C., Bralower, T.J. (Eds.), *Proc. ODP Sci. Results* 154, 83–99.
- Backman, J., Shackleton, N.J., 1983. Quantitative biochronology of Pliocene and early Pleistocene calcareous nannofossils from the Atlantic, Indian and Pacific oceans. *Mar. Micropaleontol.* 8, 141–170.
- Berggren, W.A., Kent, D.V., Swisher, C.C., Aubry, M.P., 1995. A revised Cenozoic geochronology and chronostratigraphy. *SEPM Spec. Publ.* 54, 129–212.
- Billups, K., Channell, J., Zachos, J., in press. Late Oligocene to Early Miocene paleoceanography from the Subantarctic South Atlantic (ODP Leg 177). *Paleoceanography*.
- Bukry, D., 1973. Low-latitude coccolith biostratigraphic zonation. In: Edgar, E.N.T., Saunders, J.B. et al. (Eds.), *Init. Rep. DSDP* 15, 685–703.
- Bukry, D., 1991. Paleocological transect of western Pacific Ocean late Pliocene coccolith flora. Part I. Tropical Ontong-Java Plateau at ODP Site 806B. *Open-file Rep. US Geol. Surv.* 91-552, pp. 1–35.
- Castradori, D., 1993. Calcareous nannofossil biostratigraphy and biochronology in eastern Mediterranean deep-sea cores. *Riv. Ital. Paleontol. Stratigr.* 99, 107–126.
- Censarek, B., Gersonde, R., this issue. Miocene diatom biostratigraphy at ODP Sites 689, 690, 1088, 1092 (Atlantic sector of the Southern Ocean).
- De Kaenel, E., Villa, G., 1996. Oligocene–Miocene calcareous nannofossil biostratigraphy and paleoecology from the Iberia abyssal plain. *Proc. ODP Sci. Results* 149, 79–145.
- Di Stefano, E., Sprovieri, R., Scarantino, S., 1996. Chronology of biostratigraphic events at the base of the Pliocene. *Palaeopelagos (Rome)* 6, 401–414.
- Driever, B.W.M., 1988. Calcareous nannofossil biostratigraphy and paleoenvironmental interpretation of the Mediterranean Pliocene. *Utrecht Micropaleontol. Bull.* 36, 1–245.
- Fornaciari, E., 1996. Calcareous nannofossil biostratigraphy of the California margin. *Proc. ODP Sci. Results* 167, 3–40.
- Fornaciari, E., Rio, D., 1996. Latest Oligocene to early middle Miocene quantitative calcareous nannofossil biostratigraphy in the Mediterranean region. *Micropaleontology* 42, 1–36.
- Fornaciari, E., Raffi, I., Rio, D., Villa, G., Backman, J., Olafsson, G., 1990. Quantitative distribution pattern of Oligocene and Miocene calcareous nannofossils from western equatorial Indian Ocean. *Proc. ODP Sci. Results* 115, 237–254.
- Fornaciari, E., Backman, J., Rio, D., 1993. Quantitative distribution patterns of selected Lower to Middle Miocene Calcareous Nannofossils from the Ontong Java Plateau. *Proc. ODP Sci. Results* 130, 245–256.
- Fornaciari, E., Di Stefano, A., Rio, D., Negri, A., 1996. Middle Miocene quantitative calcareous nannofossil biostratigraphy in the Mediterranean region. *Micropaleontology* 42, 37–63.
- Galeotti, S., Coccioni, R., Gersonde, R., this issue. Middle Eocene–Early Pliocene Subantarctic planktic foraminiferal biostratigraphy of ODP Leg 177 Site 1090, Agulhas Ridge.
- Gartner, S., 1988. Paleoceanography of the mid-Pleistocene. *Mar. Micropalaeontol.* 13, 23–46.
- Gartner, S., 1990. Neogene calcareous nannofossil biostratigraphy, Leg 116 (Central Indian Ocean). In: Cochran, J.R., Stow, D.A.V. et al. (Eds.), *Proc. ODP Sci. Results* 116, 165–187.
- Gartner, S., 1992. Miocene nannofossil chronology in the North Atlantic DSDP Site 608. *Mar. Micropaleontol.* 18, 307–331.
- Gartner, S., Chow, J., Stanton, R.J., Jr., 1987. Late Neogene paleoceanography of the eastern Caribbean, the Gulf of Mexico, and the eastern equatorial Pacific. *Mar. Micropaleontol.* 12, 255–304.
- Gersonde, R., Hodell, D., Blum, P. et al., 1999. *Proc. ODP Init. Rep. 177*. ODP, College Station, TX.
- Lourens, L.J., Antonarakou, A., Hilgen, J., Van Hoof, A.A.M., Vergnaud-Grazzini, C., Zachariasse, W., 1996. Evaluation of a Plio–Pleistocene astronomical time scale. *Paleoceanography* 11, 391–413.
- Maiorano, P., Monechi, S., 1998. Revised correlation of Early and Middle Miocene calcareous nannofossil events and magnetostratigraphy from DSDP Site 563 (North Atlantic Ocean). *Mar. Micropaleontol.* 35, 235–255.
- Marino, M., 1994. Biostratigrafia integrata a nannofossili calcarei e foraminiferi planctonici di alcune successioni terzogene pliocenico-superiori del Bacino di Sant'Arcangelo (Appennino meridionale). *Boll. Soc. Geol. Ital.* 113, 329–354.
- Marino, M., Flores, J.A., in press. Data report: Calcareous nannofossil stratigraphy at Sites 1088 and 1090 (ODP Leg 177, Southern Ocean). *ODP Leg 177, Sci. Results*.
- Martini, E., 1971. Standard Tertiary and Quaternary calcare-

- ous nannoplankton zonation. In: Farinacci, A. (Ed.), Proc. 2nd Int. Conf. Plankton, Rome, Vol. 2. Tecnoscienza, Rome, pp. 739–785.
- Okada, H., Bukry, D., 1980. Supplementary modification and introduction of code numbers to the low-latitude coccolith biostratigraphic zonation (Bukry, 1973; 1975). *Mar. Micropaleontol.* 5, 321–325.
- Olafsson, G., 1989. Quantitative calcareous nannofossil biostratigraphy of upper Oligocene to Middle Miocene sediments from ODP hole 667A and Middle Miocene sediments from DSDP Site 754. *Proc. ODP Sci. Results* 108, 9–22.
- Pujos, A., 1987. Late Eocene to Pleistocene medium sized and small-sized ‘Reticulofenestrids’. *Abh. Geol. Bundesanst.* 39, 239–277.
- Raffi, I., Flores, J.A., 1995. Pleistocene through Miocene calcareous nannofossils from eastern equatorial Pacific Ocean (Leg 138). *Proc. ODP Sci. Results* 138, 233–282.
- Raffi, I., Backman, J., Rio, D., Shackleton, N.J., 1993. Pliocene–Pleistocene nannofossil biostratigraphy and calibration to oxygen isotope stratigraphies from Deep Sea Drilling Project Site 607 and Ocean drilling Program Site 677. *Paleoceanography* 8, 387–408.
- Raffi, I., Rio, D., d’Atri, A., Fornaciari, E., Rocchetti, S., 1995. Quantitative distribution patterns and biomagnetostratigraphy of middle and late Miocene calcareous nannofossils from equatorial Indian and Pacific oceans (Leg 115, 130, and 138). *Proc. ODP Sci. Results* 138, 479–502.
- Rio, D., Fornaciari, E., Raffi, I., 1990a. Late Oligocene through early Pleistocene calcareous nannofossils from western equatorial Indian Ocean (Leg 115). *Proc. ODP Sci. Results* 115, 175–221.
- Rio, D., Raffi, I., Villa, G., 1990b. Pliocene–Pleistocene calcareous nannofossil distribution patterns in the Western Mediterranean. *Proc. ODP. Sci. Results* 107, 513–533.
- Samtleben, C., 1980. Die Evolution der Coccolithophoriden-Gattung *Gephyrocapsa* nach Befunden in Atlantik. *Paläontol. Z.* 54, 91–97.
- Shackleton, N.J., Baldauf, J.G., Flores, J.A., Iwai, M., Moore, T.G. Jr., Raffi, I., Vincent, E., 1995. Biostratigraphic summary for Leg 138. In: Pisias, N.J., Mayer, L.A., Janecek, T.R., Palmer-Julson, A., van Andel, T.H. (Eds.), *Proc. ODP Sci. Results* 138, 517–536.
- Shipboard Scientific Party, 1999a. Site 1088. In: Gersonde, R., Hodell, D.A., Blum, P. et al. (Eds.), *Proc. ODP Init. Rep.* 177, 1–66 (CD-ROM). Available from: Ocean Drilling Program, Texas A&M University, College Station, TX, or at www-odp.tamu.edu/publication.
- Shipboard Scientific Party, 1999b. Site 1090. In: Gersonde, R., Hodell, D.A., Blum, P. et al. (Eds.), *Proc. ODP Init. Rep.* 177, 1–101 (CD-ROM). Available from: Ocean Drilling Program, Texas A&M University, College Station, TX, or at www-odp.tamu.edu/publication.
- Shipboard Scientific Party, 1999c. Site 1092. In: Gersonde, R., Hodell, D.A., Blum, P. et al. (Eds.), *Proc. ODP Init. Rep.* 177, 1–82 (CD-ROM). Available from: Ocean Drilling Program, Texas A&M University, College Station, TX, or at www-odp.tamu.edu/publication.
- Takayama, T., 1993. Notes on Neogene calcareous nannofossil biostratigraphy of the Ontong Java Plateau and size variations of *Reticulofenestra* coccoliths. *Proc. ODP Sci. Results* 130, 179–229.
- Thiedemann, R., Sarnthein, M., Shackleton, N.J., 1994. Astronomic time scale for the Pliocene Atlantic ^{18}O and dust flux records of Ocean Drilling Program Site 659. *Paleoceanography* 9, 619–638.
- Young, J., 1990. Size variation of Neogene *Reticulofenestra* coccoliths from Indian Ocean DSDP cores. *J. Micropaleontol.* 9, 71–86.
- Young, J., 1998. Neogene. In: Bown, P. (Ed.), *Calcareous Nannofossil Biostratigraphy*. Br. Micropaleontol. Soc. Publ., London, pp. 225–265.
- Young, J., Flores, J., Wei, W., 1994. A summary chart of Neogene nannofossil magnetostratigraphy. *J. Nannoplankton Res.* 16, 21–27.